COBEM 2023 27TH INTERNATIONAL CONGRESS OF MECHANICAL ENGENEERING

ABCM Brazilian Society of Mechanical Sciences and Engineering
27th ABCM International Congress of Mechanical Engineering
December 04-08, 2023, Florianópolis-SC, Brazil

COB-2023-0997
EFFECTS OF THE PRINTING PARAMETERS ON THE SHAPE MEMORY EFFECTS ON 3D PRINTED POLYLACTIC ACID (PLA)

Brenno Tavares Duarte
Ricardo Alexandre Amar de Aguiar
Pedro Manuel Calas Lopes Pacheco
Centro Federal de Educação Tecnológica Celso Suckow da Fonseca, PPEMM, Av. Maracanã, 229 – Bloco E – 5° andar – 20271-110 – Rio de Janeiro, Brazil
brenno.duarte@cefet-rj.br, ricardo.aguiar@cefet-rj.br, pedro.pacheco@cefet-rj.br

Abstract. *Due its ability to manufacture complex structures, additive manufacturing has gained significant attention in the past decade. Particularly in the fields of prototyping; manufacturing customized parts; prosthetics and others medical applications; aerospace and automotive industries. Another exciting development on the field is four-dimensional printing (4D printing), this process allows the 3D printed material to transform to a pre-programmed shape or return to its original design given specific stimuli. This shape morphing properties are achieved through an appropriate material selection and printing conditions. To better understand and apply these shape memory polymers, several thermomechanical constitutive models have been developed over the past two decades. Fused deposition modeling (FDM), one of the most used 3D printing methods, allows for precise layer-by-layer deposition, which can affect the mechanical properties of the final product. The frequently used raw material polylactic acid (PLA) is an interesting material for 4D printing as it is a biodegradable polymer with thermo-activated shape memory behavior that allows it to be applied in a broad range of smart structures. This study aims to investigate the mechanical properties and shape memory effect of PLA polymer and the effects of the layer deposition direction on these properties. However, there is a lack of models capable of reproducing the shape memory effect in PLA polymers, these results are introduced on one constitutive model. The Tobushi model (2001), a viscoelastic model with slip conditions that the material properties are a function of the temperature. Numerical results are compared with experimental data obtained from PLA specimens to assess the applicability of these model to PLA components. These results can contribute to better geometry and printing parameters selection for controlling the mechanical properties and range of shape memory effect.*

Keywords: *Constitutive modeling, polylactic acid, 4D Printing, FDM 3D Printing Process*

1. INTRODUCTION

3D printing is an emerging technology with a growing popularity since its concept in the early 1980s (Mehrpouya, Vahabi, Janbaz, & Darafsheh, 2021), mainly due its ability to print complex shapes, fast prototyping, lower material consumption (Mehrpouya, Vahabi, Janbaz, & Darafsheh, 2021; Khalid, et al., 2022; Fu, et al., 2022). It also permits the manufacture of components with several different materials, from polymers to metal and ceramics. These remarkable characteristics enable its use on several areas that includes automotive, biomedical, electronics, product development (Mehrpouya, Vahabi, Janbaz, & Darafsheh, 2021; Khalid, et al., 2022; Fu, et al., 2022).

In 2013 the concept of four-dimensional printing was defined as spacetime 3D printed structures, i.e., 3D printed structures that changes their shape or properties when exposed to external stimulus such as heat. A good functional 4D printing design requires a selection of suitable materials that exhibit shape memory effect and are reliable for 3D printing.

Polymers are the most common 3D printing materials, accounting for about 60% of the global material used in 3D printing (Grand View Research, 2020), so it becomes natural to use shape memory polymers (SMPs) as 4D printing materials. SMPs can remember an imposed shape and return to its original shape when exposed to an activating stimulus. (Wan, Yu, & Sun, 2021) Currently, most SMPs are limited to only one-way activation (Fu, et al., 2022), that occurs due the molecular nature of polymers. The shape memory behavior of polymers is dependent on the presence of partially reversible covalent bonds or van der Waals bonds (Mehrpouya, Vahabi, Janbaz, & Darafsheh, 2021; Yarali, Taheri, & Baghani, 2020).

PLA is a largely used as 3D printing material and has compelling properties for 4D printing, such as low T_g (glass transition temperature) and shape memory effect. (Grand View Research, 2020; Mehrpouya, Vahabi, Janbaz, & Darafsheh, 2021). PLA also gains significance for its renewable sources like sugar cane or corn starch. Comparing to traditional polymers requires 65% less energy and generates 68% fewer greenhouse gases and is also biodegradable and biocompatible (Balla, et al., 2021; Ehrmann & Ehrmann, 2021). Recent studies apply 4D printing technology to the

fields of biomechanics, soft robots, adaptive metamaterials. In addition, the stimulus response speed and deformation accuracy of most current smart materials cannot meet commercial requirements. (Fu, et al., 2022)

Is necessary to accurately simulate the thermomechanical response of SMPs in order to design 4D printed elements. For this reason, since 1997 several constitutive models have been proposed to describe the SMPs behavior (Yarali, Taheri, & Baghani, 2020). They are divided into two different types of models. Rheological models based on viscoelastic models establish a relationship between the polymer-chains and spring, internal friction of the macromolecules and viscosity of the material, the sliding of polymer segments and permanent strains. In addition, these models considers that the material parameters are temperature dependent. In another approach, Phase transformation models considers the reduced molecular chains mobility at low temperatures to create two different material phases, "the frozen phase" where the sliding of polymer chains is prevented and a high temperature "active phase" where the sliding is allowed. The temperature controls the shape transformation. This transformation holds the current strain in place, generating a stored strain, when a transformation occurs from the active to the frozen phase. (Yarali, Taheri, & Baghani, 2020; Yan & Li, 2022)

Kim *et al*. (2010) proposed a model for TPU polymer that follows a more phenomenological approach which includes three phases. One viscoelastic hard phase associated chemical crosslinks maintains its mechanical properties independently of thermal inputs, and two hyperelastic soft phases acts as a shape memory switch, that can store and release the imposed strain via a reversible phase transformation.

2. CONSTITUTIVE MODEL

As there is a lack of SME constitutive models proposed for PLA materials, this study analyzes the feasibility of the Tobushi model to simulate the thermomechanical response of 4D-printed PLA specimen. The following section describes the Tobushi model.

2.1 Tobushi Model

Tobushi *et al*. (1997) proposed a uniaxial model for thin film of polyurethane (TPU) and is composed of a modified standard linear viscoelastic model with addition of a slip mechanism, as can be seen on Figure 1. The model also includes thermal expansion and is described by the following equation:

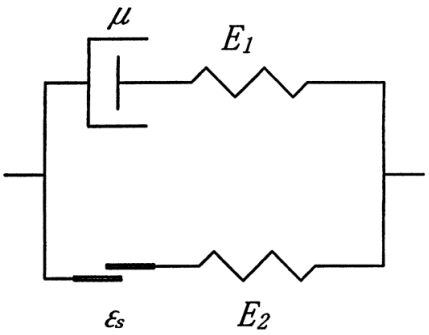

Figure 1 - Tobushi model (Tobushi, Hashimoto, Hayashi, & Yamada, 1997)

$$\dot{\varepsilon} = \frac{\dot{\sigma}}{E} + \frac{\sigma}{\mu} - \frac{\varepsilon - \varepsilon_S}{\lambda} + \alpha\dot{T} \tag{1}$$

where σ, ε and T are the stress, strain and temperature, respectively. E, μ, λ and α represents the elastic modulus, viscosity, retardation time and coefficient of thermal expansion. ε_s is the irrecoverable strain.

2.1.1 Slip Mechanism

The model includes a slip mechanism, generated by internal friction, that creates an irrecoverable strain ε_s. Where the relationship between the imposed strain ε and the irrecoverable strain ε_s is described by Eq. 2.

$$\varepsilon_S = C(\varepsilon - \varepsilon_l) \tag{2}$$

Tobushi (Tobushi, Hashimoto, Hayashi, & Yamada, 1997) explained that the slip occurs due orientation of molecular chains and decoupling of cross-link, which only appears after reach a critical value ε_l. C is a material parameter that determinates the ratio between the creep strain $(\varepsilon - \varepsilon_l)$ and the irrecoverable strain (ε_s). The shape memory effect occurs because ε_l and C are temperature dependents. At high temperatures (above T_g) the internal

friction is small resulting in large ε_l and small C. On the other hand, at low temperatures the motion of molecular chain is frozen causing higher internal friction, resulting in small ε_l and large C.

2.1.2 Thermal Dependency

To represent the shape memory effect and simulate this behavior above T_g, this model includes a temperature dependency on the materials properties and displayed on Figure 2. T_w determinates the temperature range in which the properties vary. E, μ, λ, C and $\varepsilon_l$are temperature dependent properties that follows the following equation:

$$\chi = \chi_g \exp\left[a\left(\frac{T_g}{T} - 1\right)\right] \tag{3}$$

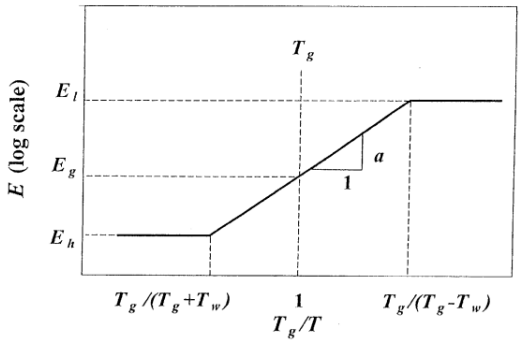

Figure 2 - Relation between temperature and mechanical properties

This linear model (Tobushi *et al.*, 1997) (Tobushi, Hashimoto, Hayashi, & Yamada, 1997) is limited to accurately represent small strains, up to 3%.

2.1.3 Non-linearity

Tobushi *et al.* (2001) proposed a few modifications to the model the model presented in the last section (Tobushi *et al.*, 1997) that includes a nonlinear time-independent strain and a nonlinear viscous effect which results in the following equation:

$$\dot{\varepsilon} = \frac{\dot{\sigma}}{E} + m\left(\frac{\sigma - \sigma_y}{k}\right)^{m-1}\frac{\dot{\sigma}}{k} + \frac{\sigma}{\mu} + \frac{1}{b}\left(\frac{\sigma}{\sigma_c} - 1\right)^n - \frac{\varepsilon - \varepsilon_S}{\lambda} + \alpha\dot{T} \tag{4}$$

where σ_y and σ_c are parameters that establishes the limits for linear behavior in the time-independent and the viscous terms, respectively. k, σ_y and σ_c parameters are temperature dependent and m, b and n parameters are constants. With these modifications Tobushi *et al.* (Tobushi, Okumura, Hayashi, & Ito, 2001) was able to simulate accurately the material behavior up to 20% strain.

3. EXPERIMENTAL PROCEDURE

The material used in this work was provided by GTMax3D, PLA in the form of 1.75 mm diameter filaments. The specimen was printed using a Core A1v2 3D printer. The printed parameters are shown in Table 1. DSC (Differential Scanning Calorimetry) and tensile tests considering different temperatures and strain rates were developed to characterize the material behavior and study the effect of printer parameters.

Table 1 - Printing parameters

Nozzle Diameter	Layer Height	Raster width	Raster Angle	Infill	Extruder Temperature	Printing bed Temperature	Printing speed
0.40 mm	0.20 mm	0.44 mm	0° and 45°	100 %	230 °C	90 °C	45 mm/s

On this study two different raster angles were used to analyze the effect of this printing parameters on the material thermomechanical behavior, as shown in Figure 3. The specimens were manufactured following the ASTM D638 (2014) type I dimensions.

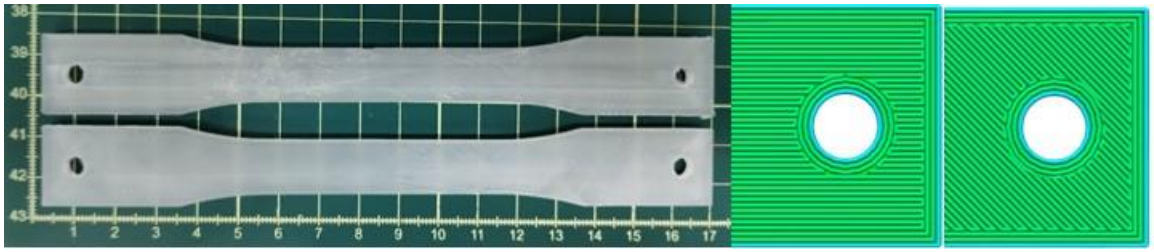

Figure 3 – Printed Specimen highlighting the deposition patern

3.1 Glass Transition

To determinate the temperatures where the glass transition starts and finish, to be used on the constitutive models, DSC tests were developed with a 15k/min heating rate in a NETZSCH DSC 200 F3 Maia. The samples were obtained from the specimen after the printing process and from the filament, to analyze any influence of the manufacturing process. Figure 4a shows similar values for the glass transition temperatures for both conditions, only a peak on the filament sample presumably due inner strain generated on its drawing process.

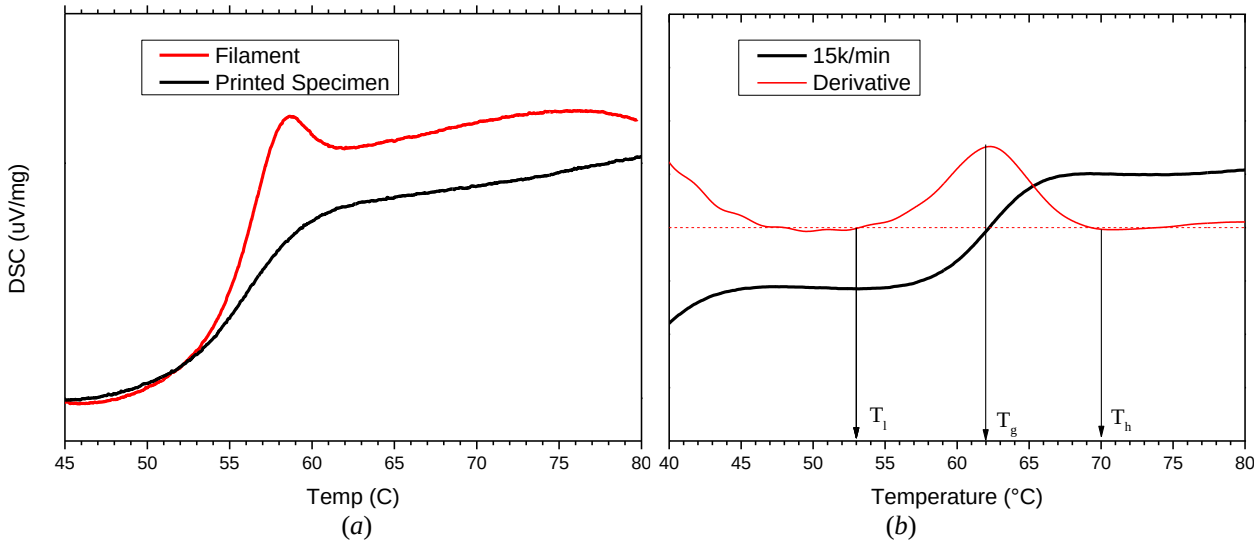

(*a*) (*b*)

Figure 4 - DSC results: (a) the filament and printed specimen; (b) Transition temperatures

The derivative of the printed specimen DSC curve was analyzed to determinate the transformations temperatures utilized on the models (Figure 4b). T_g is defined as the midpoint between T_l and T_h on the DSC curve (ASTM E-1356, 2014) or the peak on the derivative, resulting in a T_g value of 62°C. The temperatures where the transition start and finish, were selected as the temperatures where a null derivative of the curve occurs, resulting in the following values: $T_l = 53℃$ and $T_h = 70℃$

3.2 Thermomechanical Properties

To investigate the thermomechanical properties, a series of tensile tests were performed using a Instron 5982. Different strain rates were used to analyze the viscoelastic properties, with rates from 1%/min up to 50%/min. The tests were carried out to a maximum of 2.5% strain. The maximum strain adopted was set after initial tests where the specimen reached failure at about 3% strain. Figures 5 and 6 shows stress-strain curves obtained with tensile with different strain rates for lower ($T = 25℃$) and higher ($T = 70℃$) temperatures, respectively. Results shows that the specimens presents an increase in the maximum stress for higher strain rates at lower and higher temperatures. For the 0° specimen (Fig 5*a*) this behavior can only be identified at the 50%/min rate for the lower temperature.

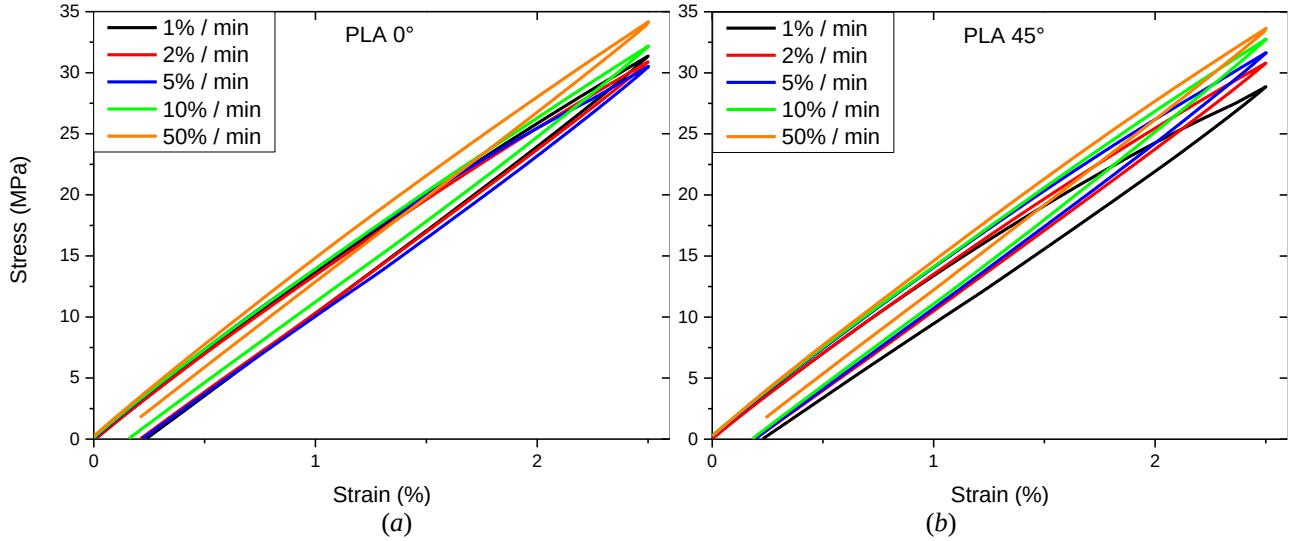

Figure 5 - Tensile tests - Strain Rate influence at $T = 25℃$: *(a)* 0° specimen *and (*b) *45*° specimen.

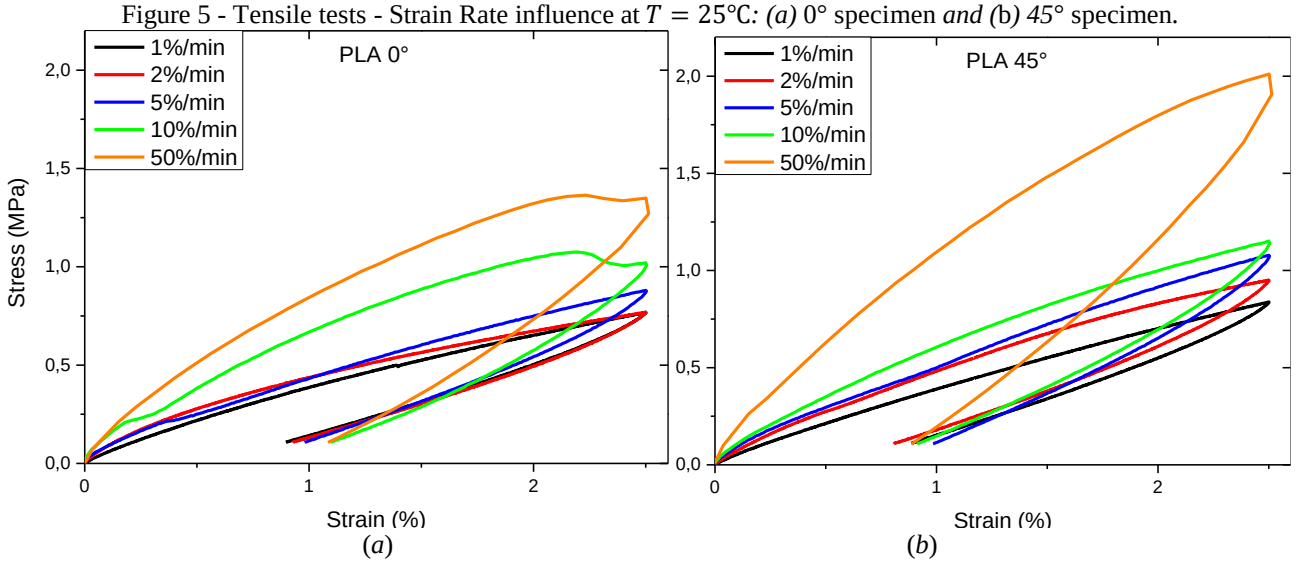

Figure 6 - Tensile tests - Strain Rate influence at $T = 70℃$: *(a)* 0° specimen *and (*b) *45*° specimen.

For analyze the temperature dependency and calibrate the temperature dependent parameters, isothermal tensile tests were carried out with low strain rate of 1%/min, to minimize viscoelastic effects. Four temperatures were defined by the DSC tests: one below T_l; two between T_l and T_h; and one above T_h. Figure 7 shows the stress-strain curves obtained with isothermal tensile tests.

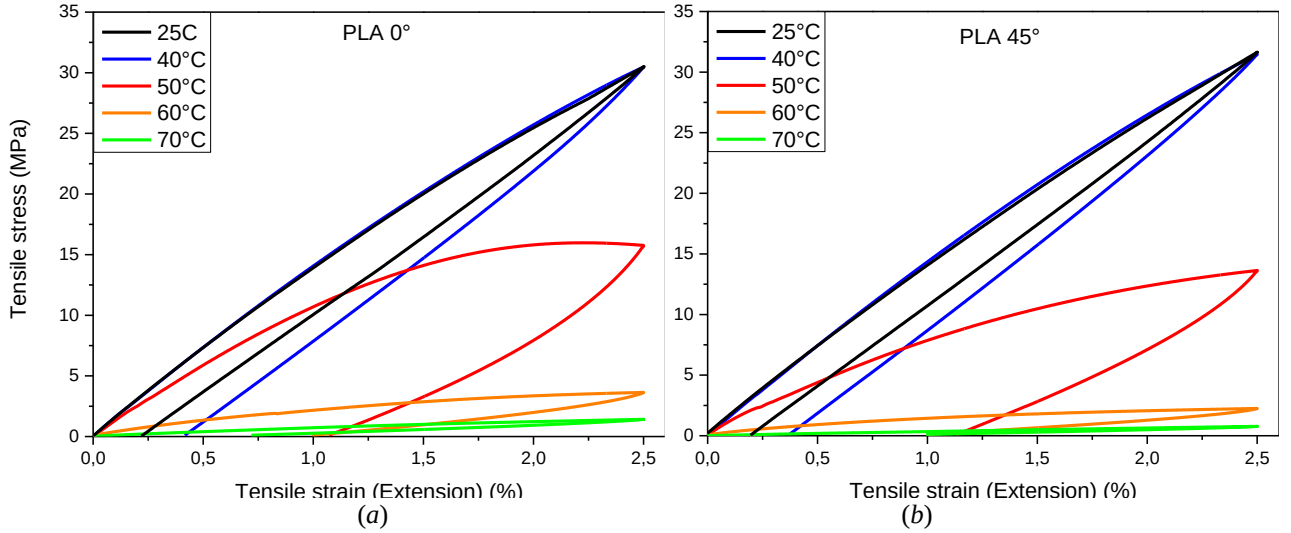

Figure 7 – Isothermal tensile tests*: (a)* 0° specimen *and (*b) *45*° specimen.

With the temperature increase, a drop on the stress is observed, that indicates a drop on the elastic modulus for the Tobushi model. To better analyze the results, Figure 8 shows the results only for the higher temperatures. The results shows that the 45° specimen has a higher stress drop when heated.

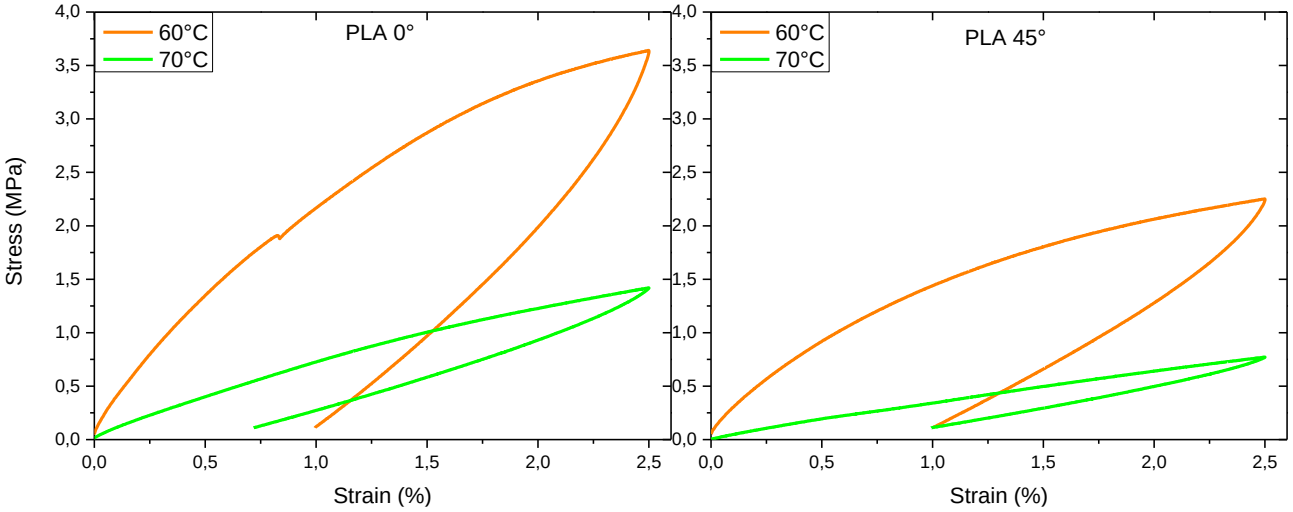

Figure 8 – Isothermal tensile tests – higher temperatures*: (a)* 0° specimen *and (*b*) 45*° specimen.

3.3 Shape Memory Effect

To verify the shape memory effect, a thermomechanical test was carried out in 4 stages: 1) the specimen in a constant temperature above T_h is submitted to a strain mechanical loading until a value of 6% strain is achieved; 2) the specimen is cooled below T_l; 3) the strain was removed in a stress control loading; 4) the specimen was heated above T_h and the temperature was maintained in a constant value. Figure 9 displays the test procedure; the red dashed lines are the regions where the stress was controlled. The thermal and strain rates adopted are 4k/min 1%/min, respectively. The vertical lines and numbered circles identify the stages of the test.

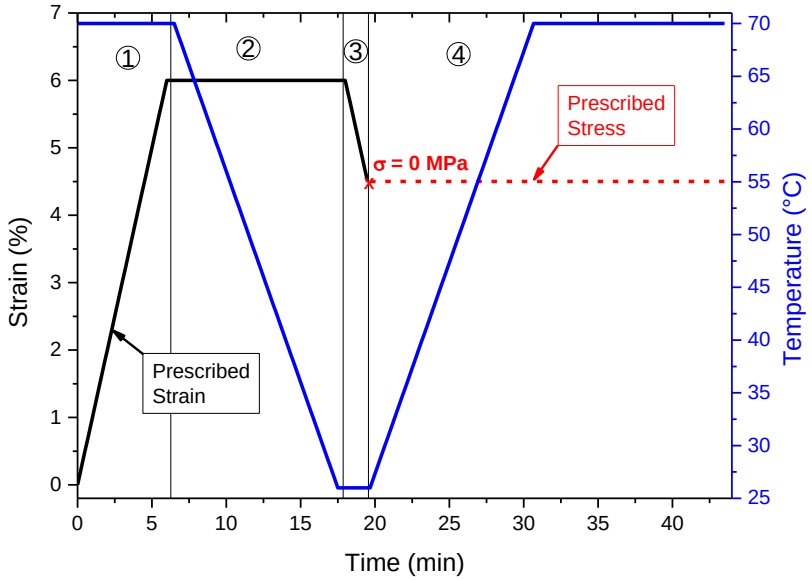

Figure 9 - Shape Memory Effect test profile. Black, red and blue lines represent the strain, stress and temperature time evolution, respectively.

Figure 10a shows the stress-strain relationship, during the test. Stress increases nonlinearly for both PLA 0° and PLA 45° specimen, but the 0° specimen reached a higher stress values. The subsequent cooling step under constant strain increases the stress, again reaching higher stress on the 0° specimen. The unloading step larger values for the elastic modulus, similar to the behavior observed on Figure 7: 1.32 GPa for PLA 0° and 1.06 GPa for PLA 45°. The

strain reached at the end of this step is the storage strain, which value is similar to both 0° and 45°. On the last heating step, the strain is released, recovering most of the imposed strain, with a higher recovery for the PLA 45°.

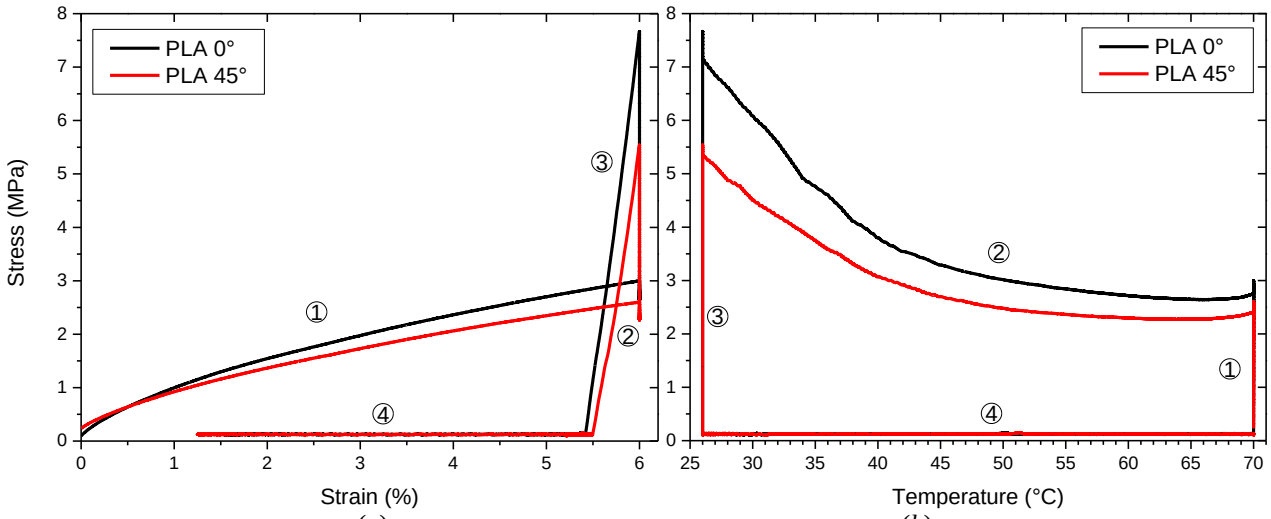

(*a*) (*b*)

Figure 10 – (a)Stress-Strain and (b) Stress-Temperature relationship on SME test for PLA 0° and PLA 45° specimen

As seen in Figure 10b, during the cooling step, the stress relaxation opposes the increasing elastic modulus and thermal contraction, resulting in an initially stable stress, but after reaching T_g the stress begins to increase. Also indicates that the PLA 0° reaches higher stress than PLA 45°, which concurs with the results displayed in Figure 8, that the PLA 45° has a larger stress drop.

The strain-temperature relationship is presented on Figure 11a. On the heating step, the strain maintains stable until reaching T_l when it begins to recover, increasing the recovery rate with higher temperatures. Both PLA 0° and 45° have similar response. There is clearly a large viscous effect on this material, with a high strain at the end of the heating step, between 3.5 and 4%. However, Figure 10a shows that the final strain on the tests are 1.54% for the 0° and 1.25% for the 45°. Figure 11b shows the delay on the strain recovery on a time response for the heating step and the final hold at T_h at a stress-free condition. Also indicates a higher recovery for the PLA 45°.

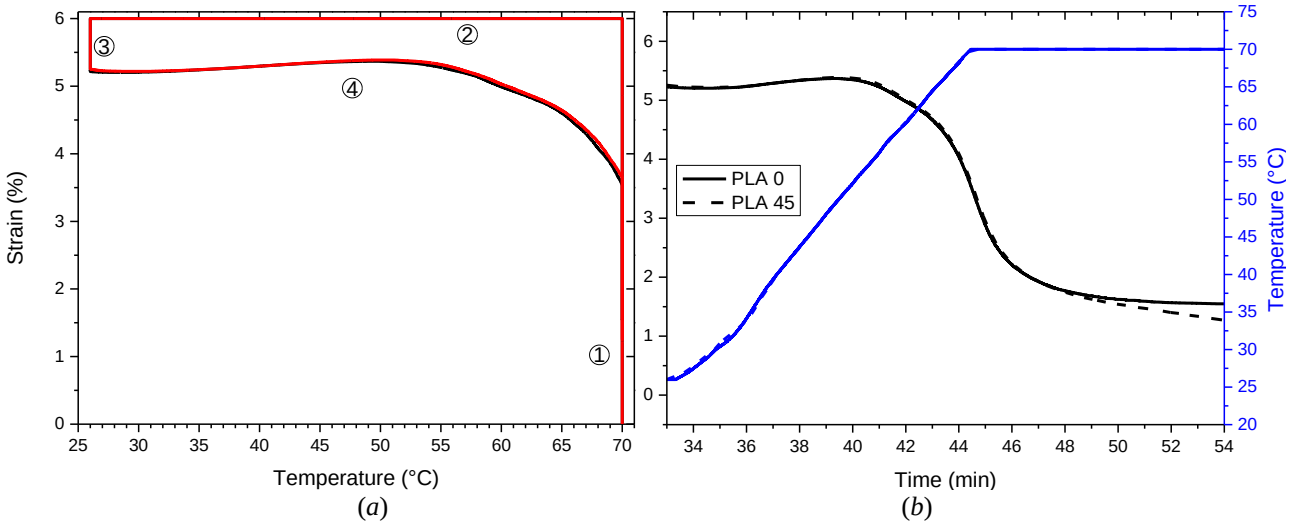

(*a*) (*b*)

Figure 11 –Strain-Temperature (a) relationship and (b) time response on SME test for PLA 0 and PLA 45 specimen

4. TOBUSHI MODEL CALIBRATION

The calibration of the Tobushi model is developed in two steps. First, parameters are calibrated for temperatures below T_f, and then for temperatures above T_h. To each temperature, at first the viscous effect is ignored to determinate the time independent parameters of Eq. 4. Then the viscous effect is reintroduced in Eq. 4 to equalize the final strain on the unloading step and adjusting the other parameters. This is done for 1%/min and 50%/min strain rates. Figure 14

displays the results for the lower temperature calibration. As can be seen from the figure, the model presents a better agreement with experimental data for PLA 0° specimen, with a 0,19% difference on the final strain. PLA 45° has a higher viscous effect (higher stress on the cyclic test and retardation time) and the model has difficulties to represent the material behavior and a 0,34% error is observed for the final strain. Figure 15 displays the calibration results for higher temperatures, and it shows that the retardation time problem is more severe with errors above 1% strain on both specimens. Table 2 shows the parameters implemented on the model.

Table 2 - PLA parameters for the Tobushi model

PLA 0°	E(MPa)	k(MPa)	σ_y (MPa)	μ (GPa s)	σ_c (MPa)	λ (s)	S (-)
$T < T_l$	1438	510	18	100	40	3000	0.6
T_g	146	40	4	35	1.5	390	0.1
$T > T_h$	110	15	0.05	5	0.9	160	0.004

PLA 45°	E(MPa)	k(MPa)	σ_y (MPa)	μ (GPa s)	σ_c (MPa)	λ (s)	S (-)
$T < T_l$	1450	440	14	110	10	2100	0.6
T_g	540	80	1	18	3	153	0.1
$T > T_h$	200	20	0.05	5	0.9	29	0.009

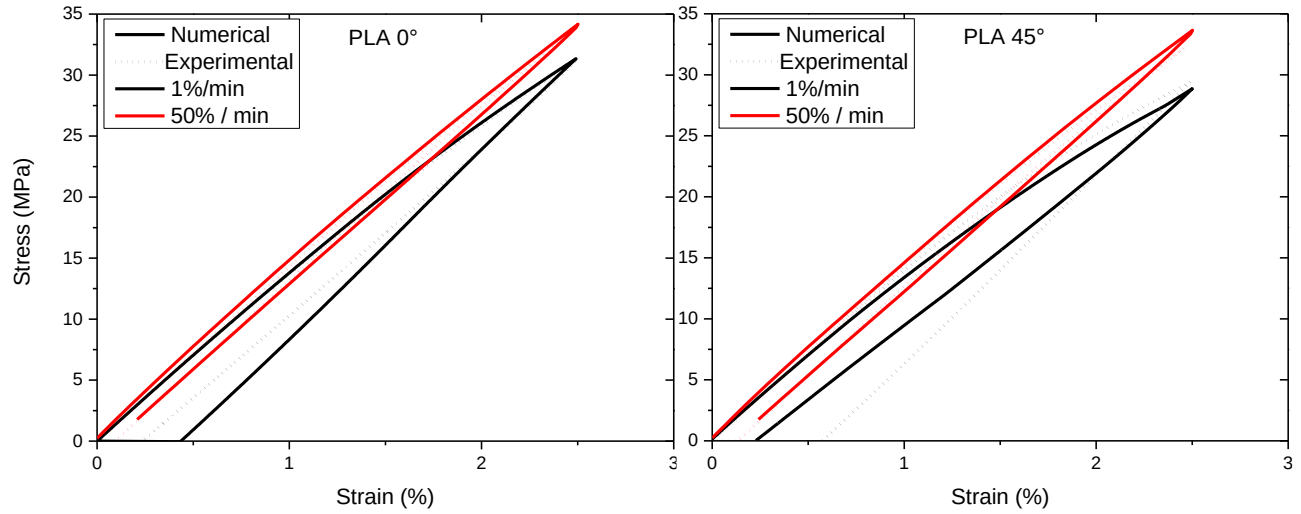

Figure 12 - Calibration of Tobushi Model below T_l: *(a)* 0° specimen *and (*b) *45*° specimen.

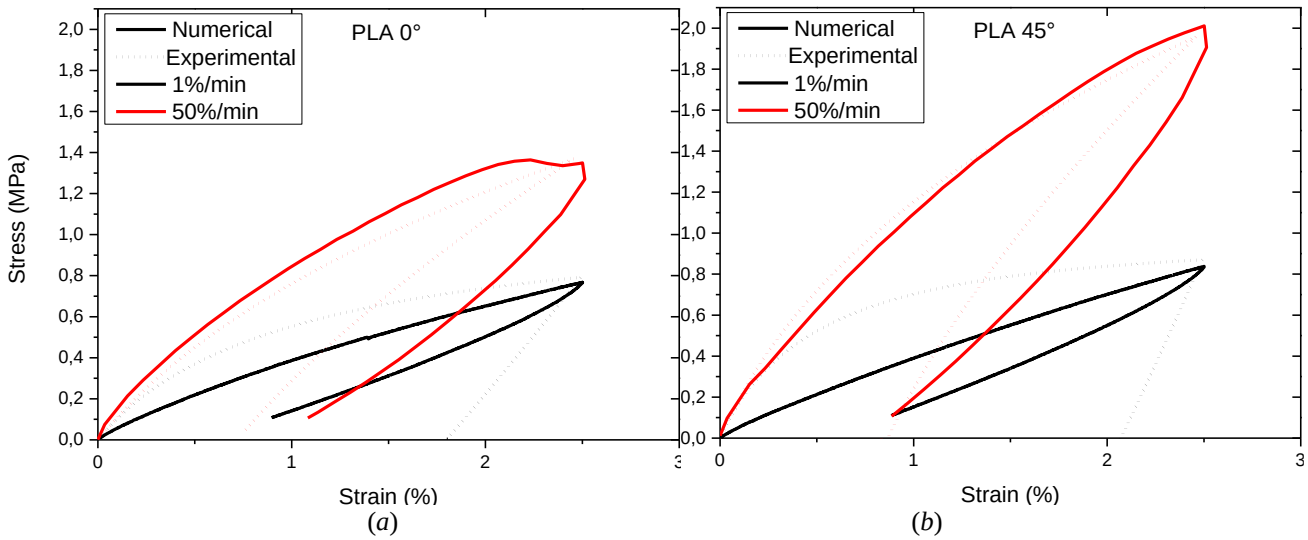

Figure 13 - Calibration of Tobushi Model above T_h: *(a)* 0° specimen *and (*b) *45*° specimen.

4.1 Shape Memory Effect

The parameters obtained in the calibration are implemented in the Tobushi model to simulate the shape memory effect considering a thermomechanical loading as described in Figure 9. Results for the PLA 45° are shown in Figure 16. As pointed in the calibration process, the Tobushi model presents some difficulties to accurately reproduce the experimental results. Figure 16a shows that the model is capable to capture the stress-strain curve behavior, with similar elastic modulus values during the unloading (1.24 GPa for the numerical and 1.06 GPa for the experimental). However, different strains are observed at the end of the test due to the initial stress on this step. During cooling prosses, Figure 16b shows that the stress increases due change in material properties and reaches a peak the at 47°C, and then decreases, indicating that the stress relaxation is prevalent on this step. Figure 16c shows that the strain during the final heating step behaves similarly but starts with higher strains, as seen on Figure 16a, and recovers a higher amount of strain.

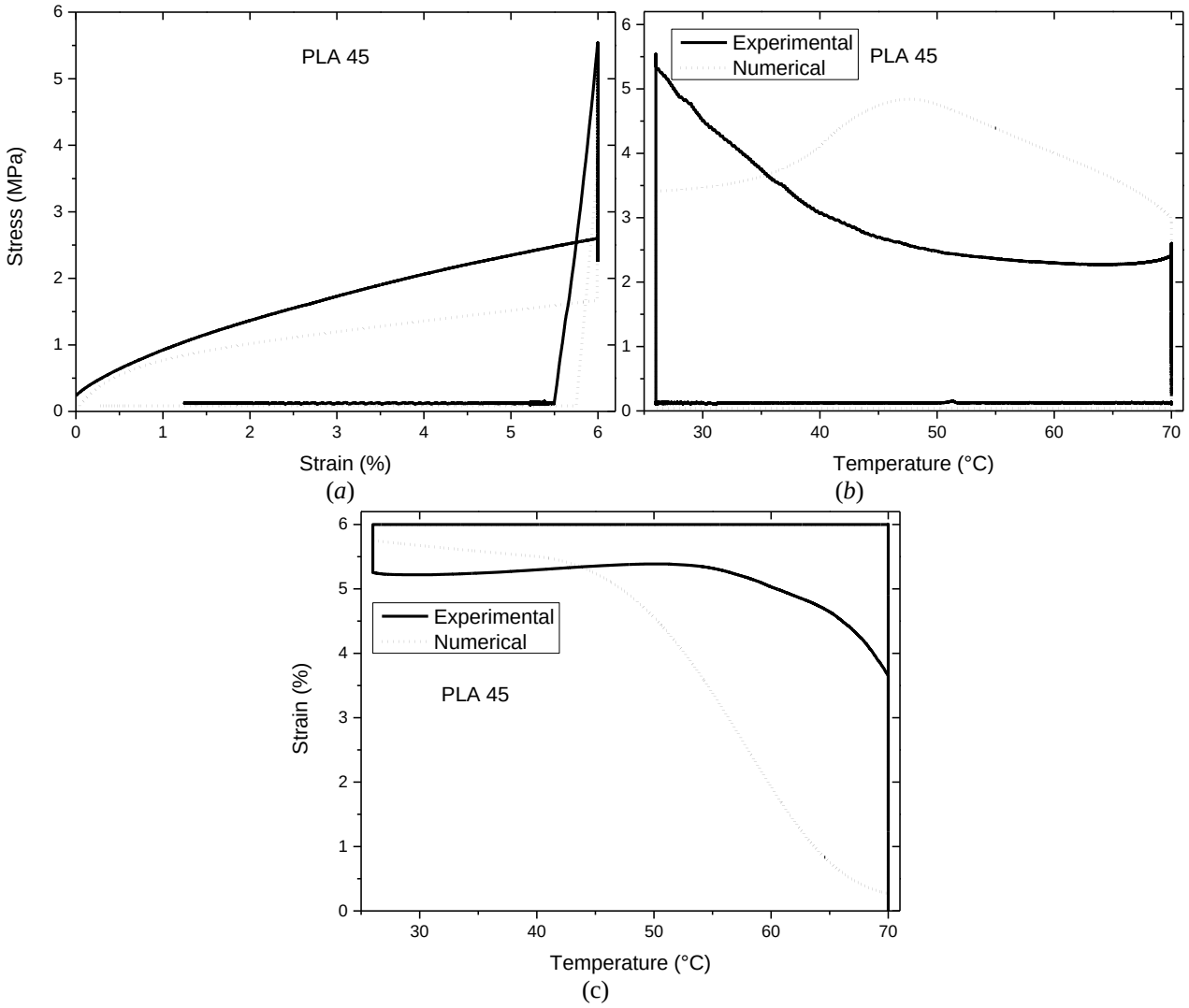

Figure 14 – Shape memory effect results for the 45° specimen: (a)Stress-Strain, (b) Stress-Temperature and (c) Strain-Temperature

5. CONCLUSION

Four-dimensional printing (4D printing) is an innovative and growing area, as it allows the use of printed material in components with a pre-programmed shape that returns to its original shape after the application of specific stimuli, such as variation in temperature. Several applications can take advantage of these special features. PLA is a largely used as 3D printing material that has compelling properties for 4D printing and presents the shape memory effect. However, these materials lack models that adequately reproduce these special properties.

In this work, experimental procedure was established to study the influence of raster angle during printing on the thermomechanical behavior of PLA polymer, considering two raster angles of 0° and 45°, and to assess the applicability to model PLA components using the Tobushi model.

DSC tests showed that the printing processed did not significantly change the glass transition temperatures. Tensile tests at lower temperatures (below T_l) showed that raster angle provided no influence on the Elastic modulus and small influence on viscoelastic behavior. On the other hand, at higher temperatures (above T_l) and small strain rates (1%/min) 45° raster specimens present approximately 36% lower stress than 0° specimen for all tests. Tensile tests indicates that 45° raster specimens are more influenced by the strain rates, reaching higher stress values than 0° specimen.

The Tobushi model was developed for TPU and present some issues to simulate the PLA thermomechanical response with different strain rates. That was expected, mainly due different thermomechanical responses from PLA and TPU. PLA has a fragile behavior at room temperature whereas TPU presents a hyperelastic behavior. Therefore, different or improved models are required to represent adequately the thermomechanical behavior of the Shape Memory Effect in PLAs. The Kim model has the capacity to define the volume fraction of each phase, so it can be a better alternative, to represent the elastic and viscoelastic properties of the material. But the model proposes all three phases to be viscoelastic or hyperelastic, so a new or modified SME model capable of represent the different mechanisms should be proposed to better represent the thermomechanical behavior of PLA.

6. ACKNOWLEDGEMENTS

The authors would like to acknowledge the support of the Brazilian Research Agencies CNPq, CAPES, and FAPERJ.

7. REFERENCES

ASTM International, 2014, *ASTM E1356 - Standard Test Method for Assignment of the Glass Transition Temperatures by Differential Scanning Calorimetry*.

ASTM International, 2014, *ASTM D638 - Standard Test Method for Tensile Properties of Plastics*.

Balla, E., Daniilidis, V., Karlioti, G., Kalamas, T., Stefanidou, M., Bikiaris, N. D., Vlachopoulos, A., and Koumentakouu, I., 2021, Poly(lactic Acid): A Versatile Biobased Polymer for the Future with Multifunctional Properties - From Monomer Synthesis, Polymerization Techniques and Molecular Weight Increase to PLA Applications. *Polymers*.

Ehrmann, G., and Ehrmann, A., 2021, Shape-Memory Properties of 3D Printed PLA Structures. In *Proceedings of The First International Conference on "Green" Polymer Materials*.

Fu, P., Li, H., Gong, J., Fan, Z., Smith, A. T., Shen, K., Khafalla, T., Huang, H., Qjan, X., McCtcheon, J., and Sun, L., 2022, 4D printing of polymers: Techniques, materials, and prospects. *Progress in Polymer Science*.

Grand View Research, 2020, *3D Printing Filament Market Size, Share & Trends Analysis Report By Type (Plastics, Metal, Ceramics), By Plastic Type (Polylactic Acid, ABS), By Application (Industrial, Aerospace & Defense), By Region, And Segment Forecasts, 2020 - 2027.*

Khalid, M. Y., Arif, Z. U., Ahmed, W., Umer, R., Zolfagharian, A., and Bodaghi, M., 2022, 4D printing: Technological developments in robotics applications. *Sensors and Actuators: A. Physical*.

Kim, J. H., Kang, T. J., and Yu, W.-R., 2010, Thermo-mechanical constitutive modeling of shape memory polyurethanes using a phenomenological approach. *International Journal of Plasticity*.

Mehrpouya, M., Vahabi, H., Janbaz, S., and Darafsheh, A., 2021, 4D printing of shape memory polylactic acid (PLA), *Polymer*.

Tobushi, H., Hashimoto, T., Hayashi, S., and Yamada, E., 1997, Thermomechanical Constitutive Modeling in Shape Memory Polymer of Polyurethane Series, *Journal of Intelligent Material Systems and Structures*.

Tobushi, H., Okumura, K., Hayashi, S., and Ito, N, 2001, Thermomechanical constitutive model of shape memory Polymers. *Mechanics of Materials*.

Wan, M., Yu, K., and Sun, H., 2021, 4D printed programmable auxetic metamaterials with shape memory effects. *Composite Structures*.

Yan, C., and Li, G., 2022, Tutorial: Thermomechanical constitutive modeling of shape memory polymers. *Journal of Applied Physics.*

Yarali, E., Taheri, A., and Baghani, M., 2020, A comprehensive review on thermomechanical constitutive models for shape memory polymers. *Journal of Intelligent Material Systems and Structures.*

8. RESPONSIBILITY NOTICE

The authors are the only responsible for the printed material included in this paper.